

A Unified Mechanism for Hydrogen Trapping at Metal Vacancies

Weiwei Xing¹, Xing-Qiu Chen^{1,*}, Gang Lu², Dianzhong Li¹, and Yiyi Li¹

¹ *Shenyang National Laboratory for Materials Science, Institute of Metal Research,
Chinese Academy of Sciences, Shenyang 110016, China and*

² *Department of Physics and Astronomy, California State University Northridge, Northridge, California 91330, USA*
(Dated: August 19, 2018)

Interaction between hydrogen (H) and metals is central to many materials problems of scientific and technological importance. Chief among them is the development of H storage and H-resistant materials. H segregation or trapping at lattice defects, including vacancies, dislocations, grain boundaries, etc, plays a crucial role in determining the properties of these materials. Here, through first-principles simulations, we propose a unified mechanism involving charge transfer induced strain destabilization to understand H segregation behavior at vacancies. We discover that H prefers to occupy interstitials with high pre-existing charge densities and the availability of such interstitials sets the limit on H trapping capacity at a vacancy. Once the maximum H capacity is reached, the dominant charge donors switch from the nearest-neighbor (NN) to the next-nearest-neighbor (NNN) metal atoms. Accompanying with this long-range charge transfer, a significant reorganization energy would occur, leading to instability of the H-vacancy complex. The physical picture unveiled here appears universal across the BCC series and is believed to be relevant to other metals/defects as well. The insight gained from this study is expected to have important implications for the design of H storage and H-resistant materials.

PACS numbers: 61.72.J-, 61.72.S-, 71.15.Mb, 71.15.Nc

Interaction between H and lattice defects underlies diverse materials phenomena [1–4], including H storage [3, 5], H embrittlement [6–8], metallic H membranes [9], nuclear fusion reactors [10, 11] and H-assisted superabundant vacancy formation in metals [1, 12, 13], etc, to name a few. Crucial to all these problems is trapping of H at the lattice defects, such as vacancies, voids, dislocations, grain boundaries and cracks [14–22]. In particular, H trapping at vacancies has attracted the most attention thanks to the facts that (1) vacancies are easier to study than other defects but have profound influences on materials properties; (2) vacancies hold many surprises and mysteries yet to be explored; (3) the insight gained from vacancies can be applied to other defects as well.

It is found that for BCC and FCC metals, up to six H atoms can be trapped by a monovacancy in general because H prefers to occupy the six octahedral (O) interstitials surrounding the vacancy [1, 16, 17]. However, there are exceptions - the maximum H capacity can go up to 10 for Molybdenum (Mo) [16, 17, 23] and 12 for Tungsten (W) and Aluminum (Al)[14]. Different interpretations of the available experimental results have also been put forward: (i) The competition between metal-H hybridization and the Coulombic repulsion determines the position and number of H atoms at the vacancy in BCC-Fe [24]; (ii) Comparing to Fe, the greater H trapping capacity in Al is attributed to a larger lattice constant and more delocalized electronic states [14]; (iii) In W, it is found that the vacancy provides an isosurface of optimal charge density that facilitates the formation of H bubbles [25]. Clearly, an important question to ask is whether there exists a unified mechanism of H trapping in metals?

In this paper, we propose such a unified mechanism based on quantum-mechanical density functional theory (DFT) calculations. We show that charge transfer induced strain destabilization is responsible for H trapping behavior at vacancies across the BCC series. By examining H trapping at monovacancies in these BCC metals (including V, Nb and Ta as good candidates for H storage; Mo and W as the most promising plasma facing materials of nuclear fusion reactors, and Fe and Cr as the most commonly used elements in H-resistant structural steels), we discover that H prefers to occupy the interstitials with high pre-existing charge densities with or without a vacancy. The availability of such interstitials determines the H capacity at a vacancy. When the maximum H capacity is reached, the dominant charge donors switch from the NN to the NNN metal atoms. The long-range charge transfer leads to a significant strain energy cost. The correlation between the charge transfer and the onset of mechanical “instability” appears universal across the BCC series, and ultimately determines the limit on H storage in metals.

The DFT calculations were carried out using Vienna *ab initio* Simulation Package(VASP)[29–31] with the projector augmented wave potential(PAW) method [32, 33] and the generalized gradient approximation (GGA) of Perdew-Burke-Ernzerhof(PBE)[34] form was employed for electron exchange and correlation. An energy cut-off of 400eV was chosen for the plane-wave expansion of eigenfunctions. All results were obtained with a 54-atom supercell; for Ta, Mo and W, a 128-atom supercell was also used to check the convergence of the results. The difference in H trapping energies between the 128-atom and 54-atom supercells is less than 0.03 eV, confirming

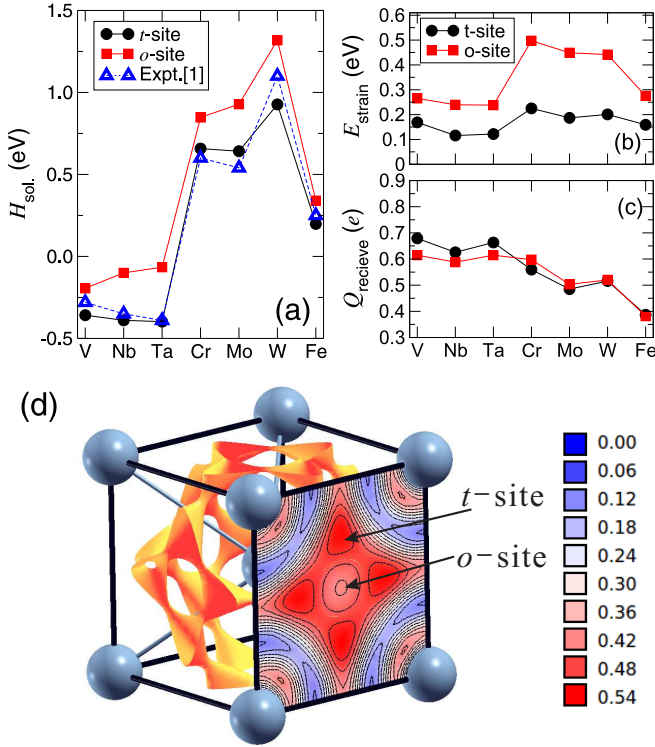


FIG. 1: H in defect-free metals. (a) The solution enthalpies (along with available experimental data [1]) of H, (b) the strain energy induced by H insertion and (c) the received charges of H at **T** or **O**-sites in seven BCC-type metals (V, Nb, Ta, Cr, Mo, W, and Fe). (c) Isosurface (with an isovalue of 0.42) of the electron localized function (ELF) and its contour plot on (001) plane showing the highest charge densities at the **T**-sites in V. The similar results have been observed for other six BCC metals (Cr, Fe, Nb, Mo, Ta and W), but are not shown here.

our results are converged. The Brillouin-zone integrations were performed by using a $4 \times 4 \times 4$ k-mesh for 54 atoms and $3 \times 3 \times 3$ k-mesh for 128 atoms according to the Monkhorst-Pack scheme.[35] Spin polarized calculations were performed for Cr and Fe although the magnetism only slightly affects the properties of Cr-H system.[17] We did not consider zero-point energy (ZPE) correction in the calculations for the same reason as explained in Ref. [16, 17, 24, 25].

To determine the strain energy of the $\text{vac-}n\text{H}$ complexes, we remove H atoms and compute the total energies of H-free vacancy with and without relaxing the metal atoms. The strain energy is defined as the total energy difference before and after the relaxation: $E_{\text{strain}}(\text{vac-}n\text{H}) = E_{\text{hollow}}^{\text{unrelaxed}} - E_{\text{hollow}}^{\text{relaxed}}$. The differential strain energies is defined as the strain energy difference between $\text{vac-}(n+1)\text{H}$ cluster and $\text{vac-}n\text{H}$ cluster: $\Delta E_{\text{strain}} = E_{\text{strain}}(\text{vac-}(n+1)\text{H}) - E_{\text{strain}}(\text{vac-}n\text{H})$. The differential strain energy represents the change in the strain energy induced by an additional H atom incor-

porated to the $\text{vac-}n\text{H}$ cluster.

The charge deficit on the nearest-neighbor (NN) and the next-nearest-neighbor (NNN) metal atoms surrounding the vacancy can be estimated by the following equation: $Q_{\text{losing}}^X = \Sigma[Q_{\text{vac-}n\text{H}}^X(\text{Tm}) - Q_{\text{vac}}^X(\text{Tm})]$, where X denotes the NN or NNN atoms surrounding the monovacancy, and $Q_{\text{vac-}n\text{H}}$ and Q_{vac} refer to the charges of the NN or NNN atoms after and before the trapping of H, respectively.

H trapping in a perfect lattice In defect-free BCC metals considered here, we reproduce the known fact that H prefers the tetrahedral interstitial (**T**) to the octahedral interstitial (**O**), as evidenced in Fig. 1a. The solution enthalpies of H at the **T**-sites are in excellent agreement with the experimentally measured data in the low concentration limit of H [1], verifying the reliability of our DFT calculations. To our surprise, the strain energy induced by H occupying the **O** interstitial is much higher than the **T** interstitial (*c.f.*, Fig. 1b). Being smaller than the interstitial volume, H is not expected to yield substantial strain energy difference between the **T** and **O** sites [11]. Thus the result suggests that there is more to H trapping than a simple consideration of size effect. Indeed, an inspection of the charge density plot in Fig. 1d reveals a surprising clue. The contours of the electronic localization function (ELF) [26] indicate that the **T** interstitials exhibit the highest charge density with an ELF of 0.54, much larger than that at the **O** interstitials with an ELF of 0.28. More interestingly, this observation appears universal across BCC series examined here. Utilizing the Bader's technique [27], we find that H atoms trapped at both interstitials attract electrons from the host atoms in nearly the same amount (see Fig. 1c). Because the pre-existing charge density at the **O** interstitials is much lower than that at the **T** interstitials, transferring the same amount of charge to the H atoms at the **O** sites would lead to a higher strain energy, thereby rendering the **O**-sites less favorable. The fact that the most favorable H trapping sites coincide with the highest pre-existing charge density across the BCC series suggest that the charge accumulation plays a crucial role in H trapping.

H trapping at vacancies When a vacancy, the most common defect, is introduced in metals, the trapping behavior of H is quite different from that in defect-free metals [1, 14, 16, 17, 24, 25]. Here, we denote a H-vacancy complex as $\text{vac-}n\text{H}$ in which n denotes the number of segregated H atoms at the monovacancy. As illustrated in Fig. 2(a and b), we reproduce well the previous findings [16, 17] for seven BCC metals. A maximum of six H atoms can be trapped at a monovacancy in V, Nb, Ta, Cr and Fe (group I), whereas up to 12 H atoms can be accommodated at a monovacancy in Mo and W (group II).

Charge transfer induced strain destabilization To elucidate H trapping behavior at vacancies, we choose V with

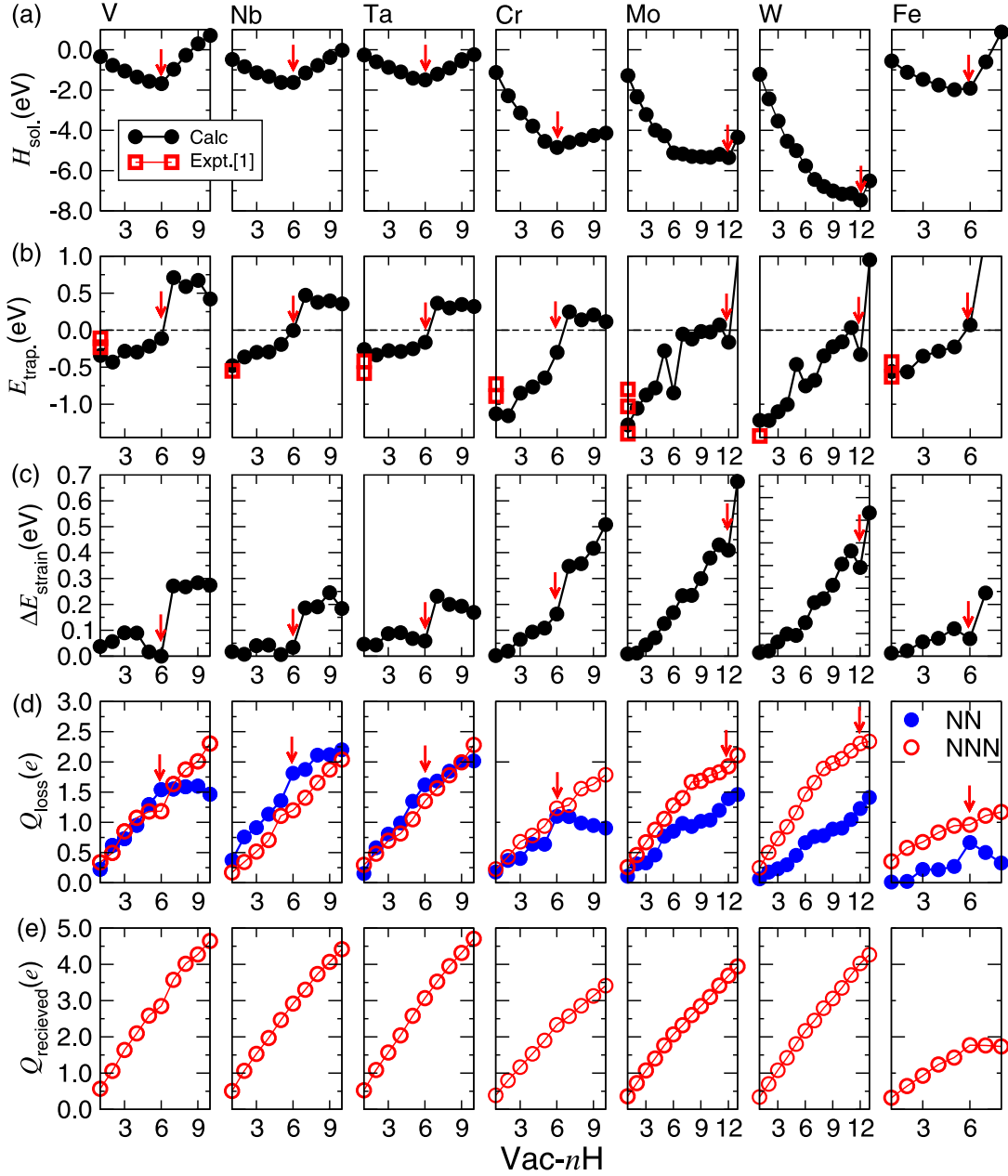


FIG. 2: H trapping at a monovacancy across the BCC series. (a) Solution enthalpies H_{sol} , (b) H trapping energies (along with available experimental data), (c) the differential strain energies, (d) the charge transfer from the eight NN (solid circles) and the six NNN (hollow circles) metal atoms, and (e) the received charges on H as a function of the number of H. Note that, in panel (b) the zero enthalpy corresponds to the energy of an interstitial H at a tetrahedral site as far as possible from the vacancy. In panel (b) we also list the experimental trapping energies for V (-0.11 eV and -0.23 eV), Fe (-0.63 eV and -0.43 eV), Ta (-0.42 eV), Mo (-1.03 eV and -0.80 eV) and W (-1.43 eV) measured by the ion implantation/channeling method, Cr (-0.89 eV and -0.73 eV) measured by the superabundant vacancy formation/thermal desorption spectroscopy, and Nb (-0.55 eV), Mo (-1.4 eV) and Ta (-0.58 eV) measured by the positron annihilation spectroscopy [1, 2]. Although the exact number of H at the vacancies was uncertain in the experiments [1, 2], the measured data are generally in a good agreement with the simulation results.

more localized $3d$ electronic states and W with less localized $5d$ states as examples to analyze the charge distribution. In Fig. 3, we display the ELF contours on (200) plane for V and W. For V, we find that the highest charge density occurs at **O** and **T**-sites, similar to

the defect-free case. In particular, the six **O** sites surrounding the vacancy now have approximately the same (high) charge density as the **T** sites. The same result is also found for other group I metals (Nb, Ta, Cr and Fe). In contrast, for group II metals (Mo and W), the

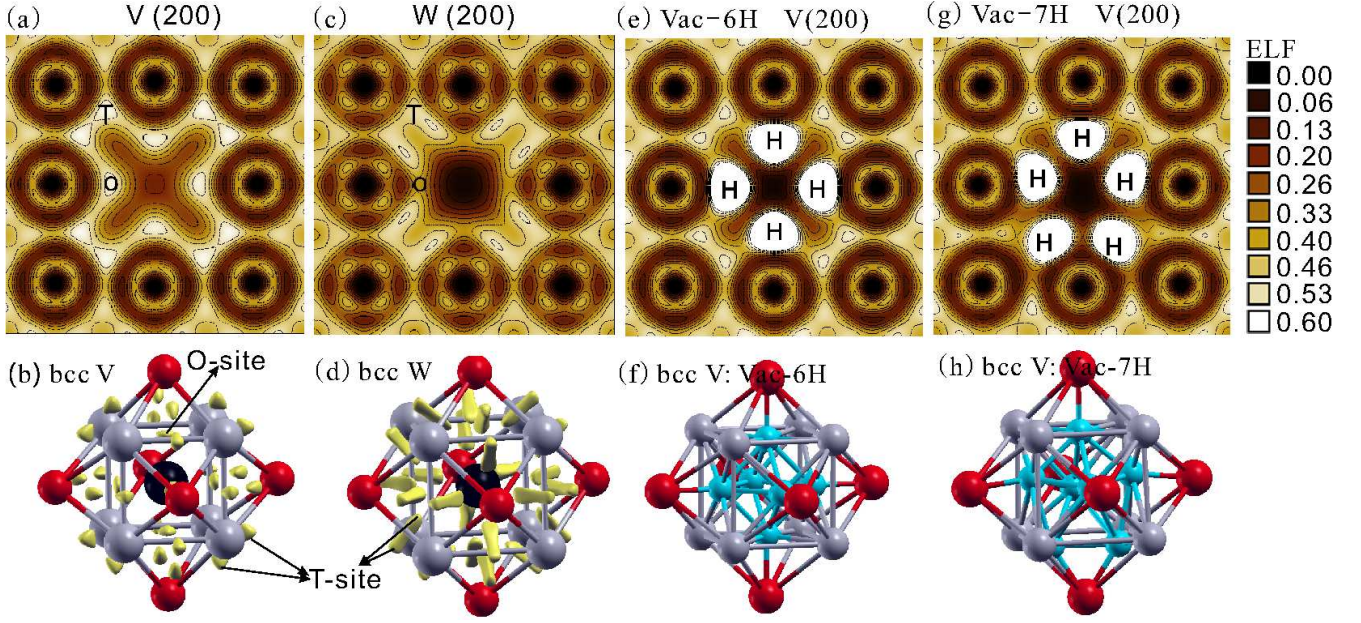


FIG. 3: The change of charge density at the interstitials before and after H is introduced in V and W. The contours of the electron localization functions (ELFs) for the (200) plane and the atomic structure surrounding the vacancy. Panels (a,b): pure V; Panels (c,d): pure W; Panels (e,g): six H atoms are trapped at the vacancy (vac-6H) in V; Panels (f,h): seven H atoms at the vacancy leading to instability in V. The 3D ELF isosurfaces in V (with an isovalue of 0.55) in Panel (b) and W (with an isovalue of 0.41) in Panel (c) evidence the vacancy-induced highest charge accumulations at the interstitial *o*- or *t*-sites for the H-free cases. The large black, grey, red and green spheres denote the vacancy, the NN, NNN metal atoms and the trapped H atoms, respectively.

highest charge density takes place at twelve equivalent tube-like regions connecting the NN *T*-sites as shown in Fig. 3(c,d)).

Similar to the defect-free case, H is also found to occupy the interstitials with the highest charge densities. For V, up to six H atoms can be accommodated at a vacancy and they occupy the six *O*-sites with the highest pre-existing charge density as shown in Fig. 3(e,f). When the seventh H atom is introduced, all atoms have to reorganize themselves; this reorganization proceeds in such a way that additional interstitials with high charge densities, such as the nearby *T*-sites, become available to H occupation. Since the *T*-sites are inequivalent from the *O*-sites, occupation of these *T* sites would introduce distortion to the lattice. Indeed as shown in Fig. 2c, there is a jump of the strain energy at $n = 7$. In fact, this sudden increase in the strain energy is observed for all group I metals. Moreover, this charge transfer induced strain destabilization is also found for Mo and W of the group II. As shown in Fig. 2(a-d), the similar jump in the strain energy is evident for $n = 13$. In this case, H occupation at additional interstitials beyond the twelve cylinder-like sites leads to lattice distortion and increases the strain energy. This observation underlies the fact that up to twelve H atoms can be trapped at a vacancy in the group II metals.

As displayed in Fig. 2(e), the total charges that the vac- n H complexes received are monotonously increased as a function of n . Obviously, the transferred charges have to mainly originate from the metallic atoms surrounding the vacancy, including eight NN atoms and six NNN atoms. Whereas the transferred charges from the NNN atoms increase monotonously as n across the BCC series, the charge transfer from the NN atoms initially increase, but after a kink (as marked by arrows in Fig. 2(d)) at $n = 6$, it starts to decrease for the group I metals, V, Cr and Fe. Although not as obvious as in V, Cr and Fe, the similar trend can be also found at $n = 6$ for Ta and Nb in the group I. Interestingly, the kink appears at $n = 6$, corresponding to the maximal H capacity for the group I metals. Hence the declining charge transfer from the NN atoms gives rise to the instability of the vacancy- n H complex. In contrast, such kinks are not observed for the group II metals.

For the type-I group, the charge transfer to H is relatively more difficult due to more localized nature of the electron states. In this case, the charge transfer from the NNN atoms becomes increasingly important as the H-vacancy cluster grows. For some instances, with the increasing charge transfer from the NNN atoms, the charge contribution from the NN atoms starts to decrease, leading to the kink as observed at $n=6$. However, this long-

range charge transfer from the NNN atoms yields a higher reorganization energy. Therefore, the kink in the charge transfer also coincides with the sharp increase of the strain energy and the onset of the instability. For the group II, the charge transfer not only stems from the NN atoms but also the NNN atoms thanks to the more delocalized nature of electronic states. Thus there is an obvious transition from the NN atoms to the NNN atoms as in the group I, and no apparent kinks in the charge transfer for the group II.

Finally, we note that H also prefers to occupy the interstitials with high pre-existing charge density in other types of lattice defects, such as grain boundaries [36], dislocations [36, 37], and cracks [38]. We have also revisited the case of FCC Al and the similar charge transfer induced strain destabilization is also observed. This universal behavior of H occupation at defects accentuates the importance of the proposed mechanism in understanding H segregation in metals.

In summary, we find that H prefers to occupy interstitials with high pre-existing charge densities. The charge transfer induced strain destabilization is responsible for the maximum H storage in BCC and possibly other metals. The insights gained from the study could provide guidance in the design of H storage or H-resistant materials. Strain engineering, defect engineering and alloying could be effective means to modify the charge density distribution at the defects, thereby changing the H concentration in the material.

Acknowledgements This work was supported by the “Hundred Talents Project” of the Chinese Academy of Sciences and from the Major Research Plan (Grand Number: 91226204) of the National Natural Science Foundation of China (Grand Numbers: 51074151 and 51174188) and Beijing Supercomputing Center of CAS (including its Shenyang branch) and Vienna Scientific Clusters.

* Corresponding author: xingqiu.chen@imr.ac.cn

- [1] Y. Fukai, *The Metal-Hydrogen System: Basic Bulk Properties*, 2nd edn (Springer, 2005).
- [2] S. M. Myers, M. I. Baskes, H. K. Birnbaum, J. W. Corbett, G. G. Deleo, S. K. Estreicher, E. E. Haller, P. Jena, N. M. Johnson, P. Kirchheim, S. J. Pearton and M. J. Stavola, *Rev. Mod. Phys.*, **64**, 559–617 (1992).
- [3] B. Sakintuna, F. Lamari-Darkrim, and M. Hirscher, *Int. J. Hydrogen Energy*, **32**, 1121–1140 (2007).
- [4] W. H. Johnson, *Proc. R. Soc. Lond.*, **23**, 168–175 (1875).
- [5] P. Chen, Z. T. Xiong, J. Z. Luo, J. Y. Liu, and L. K. Tian, *Nature* (London), **420**, 302–304 (2002).
- [6] J. Song and W. A. Curtin, *Nature Mat.*, **12**, 145–151 (2013).
- [7] R. A. Oriani, *Ber. Bunsenges. Phys. Chem.* **76**, 848–857 (1972).
- [8] J. Von. Pezold, L. Lymperakis, and J. Neugebauer, *Acta Mater.* **59**, 2969–2980 (2011).
- [9] S. Adhikari and S. Fernando, *Ind. Eng. Chem. Res.*, **45**, 875–881 (2006).
- [10] V. Barabash, The ITER International Team, A. Peacock, S. Fabritsiev, G. Kalinin, S. Zinkle, A. Rowcliffe, J. -W. Rensman, A. A. Tavassoli P. Marmy, P. J. Karditsas, F. Gillemot, and M. Akiba, *J. of Nucl. Mater.*, **367–370**, 21–32 (2007).
- [11] H.-B. Zhou, S. Jin, Y. Zhang, G.-H. Lu, and F. Liu, *Phys. Rev. Lett.*, **109**, 135502 (2012).
- [12] Y. Fukai, *Phys. Scr.*, **T103**, 11–14 (2003).
- [13] Y. Fukai and N. Okuma, *Phys. Rev. Lett.*, **73**, 1640–1643 (1994).
- [14] G. Lu and E. Kaxiras, *Phys. Rev. Lett.*, **94**, 155501 (2005).
- [15] P. R. Monasterio, T. T. Lau, S. Yip, and K. J. Van Vliet, *Phys. Rev. Lett.*, **103**, 085501 (2009).
- [16] K. Ohsawa, J. Goto, M. Yamakami, M. Yamaguchi, and M. Yagi, *Phys. Rev. B*, **82**, 184117 (2010).
- [17] K. Ohsawa, K. Eguchi, H. Watanabe, M. Yamaguchi, and M. Yagi, *Phys. Rev. B*, **85**, 094102 (2012).
- [18] X. Zhang, and G. Lu, *Phys. Rev. B*, **77**, 174102 (2008).
- [19] G. Lu, Q. Zhang, N. Kioussis, and E. Kaxiras, *Phys. Rev. Lett.* **87**, 095501 (2001).
- [20] S. Wang, N. Hashimoto, Y. M. Wang, and S. Ohnuki, *Acta Mater.*, **61**, 4734–4742 (2013).
- [21] J. P. Chateau, D. Defafosse and T. Magnin, *Acta Mater.*, **50**, 1507–1522 (2002).
- [22] S. Wang, K. Takahashi, N. Hashimoto, S. Isobe and S. Ohnuki, *Scripta Mater.* **68**, 249–252 (2013).
- [23] C. Y. Ouyang and Y. S. Lee, *Phys. Rev. B*, **83**, 045111 (2011).
- [24] Y. Tateyama and T. Ohno, *Phys. Rev. B*, **67** 174105 (2003).
- [25] Y.-L. Liu, Y. Zhang, H.-B. Zhou and G.-H. Lu, *Phys. Rev. B*, **79**, 172103 (2009).
- [26] B. Silvi and A. Savin, *Nature* (London) **371**, 683–687 (1994).
- [27] W. Tang, E. Sanville, and G. Henkelman, *J. Phys.: Condens. Matter* **21**, 084204 (2009).
- [28] A. J. Maeland and G. G. Libowitz, *J. Less Common Met.*, **74**, 295–300 (1980).
- [29] G. Kresse and J. Hafner, *Phys. Rev. B*, **48**, 13115 (1993).
- [30] G. Kresse and J. Furthmüller, *Comput. Mater. Sci.*, **6**, 15–50 (1996).
- [31] G. Kresse and J. Furthmüller, *Phys. Rev. B*, **54**, 11169–11186 (1996).
- [32] P. E. Blöchl, *Phys. Rev. B*, **50**, 17953–17979 (1994).
- [33] G. Kresse and D. Joubert, *Phys. Rev. B*, **59**, 1758–1775 (1999).
- [34] J. P. Predew and K. Burke and M. Ernzerhof, *Phys. Rev. Lett.*, **77**, 3865–3868 (1996).
- [35] H. J. Monkhorst and J. D. Pack, *Phys. Rev. B*, **13**, 5188–5192 (1976).
- [36] X. Zhang, Q. Peng and G. Lu, *Phys. Rev. B*, **82**, 134120 (2010).
- [37] G. Lu, E. B. Tadmor and E. Kaxiras, *Phys. Rev. B*, **73**, 024108 (2006).
- [38] Y. Sun, Q. Peng and G. Lu, *Phys. Rev. B*, **88**, 104109 (2013).